Involvement of Bone Marrow Stem Cells in Periodontal Wound Healing

Li Li ZHOU[1], Hong Wei LIU[1], Xin Xin WEN[1], Han XIE[1]

Objects: *To test the hypothesis whether bone marrow stem cells (BMSCs) could migrate into the periodontium as the precursor available for the repair of tissue injury.*
Methods: *A chimeric mouse model was established by transplanting BMSCs derived from red fluorescent protein mouse into irradiated BALB/c mice. Subsequently, a periodontal defect was created beside the maxillary first molar and filled with ceramic bovine bone. Finally, the chimeric mice were divided into three groups and were observed 3, 14 and 28 days later respectively. The involvement of BMSCs in periodontal defects was analysed using an* in vivo *imaging system and immunohistochemical staining of CD45, CD105 and CD31. Cell surface marker expression in injured tissue was also compared with that in normal tissue.*
Results: *Increasing numbers of BMSCs migrated into the periodontal defect with time. The distribution was initially limited to ceramic bovine bone and then around blood vessels and near alveolar bone. Furthermore, expression of CD105 and CD31 was much higher in injured periodontal tissue than that in healthy periodontium, although CD45 was not expressed in either of these tissues.*
Conclusion: *BMSCs, but not haemopoietic stem cells, were involved in periodontal defect; they entered the periodontium probably via blood vessels.*

Key words: *bone marrow stem cell (BMSC), red fluorescent protein (RFP), periodontal ligament stem cell (PDLSC)*

Currently, periodontitis remains an irreversible disease involving loss of attachment levels and supporting alveolar bone[1]. This disease is extremely common and, in spite of its prevailing incidence, no effective dental therapy is available for periodontal regeneration. Over past decades, the treatment of periodontitis has relied mainly on traditional clinical strategies, such as scaling and root planing and guided tissue regeneration. Although these measures mediate beneficial effects, such as the improvement of attachment level loss and alveolar bone absorption, the capacity to restore the physiological architecture of the original periodontium is limited[2] and these methods do not address the basic problems. However, recently, more attention has been focused on periodontal tissue engineering, which is considered to be a promising way to achieve complete, reliable and reproducible periodontal regeneration[3]. Tissue engineering comprises three components: seed cells, signal molecules and scaffolds[4]. Thus, seed cells play a significant role in periodontal regeneration. Seo (2004)[5] demonstrated the existence of stem cells in the periodontal ligament (PDL), as well as their potential periodontal tissue lineage differentiation capacity. However, the origin of these cells remains to be elucidated. During tooth development, stem cells in the periodontium are believed to originate from ancestral cells in the dental follicle[6-9], although the origin of renewed periodontal ligament stem cells (PDLSCs) after tooth development is still unknown. Bone marrow stem cells (BMSCs) share similar characteristics with PDLSCs[5,10,11] and is contributed to periodontal regeneration[12-14]. Conse-

1 Department of Periodontology, Laboratory of Oral Biomedical Science and Translational Medicine, School of Stomatology, Tongji University, Shanghai, P.R. China.

Corresponding author: Dr. Hong Wei LIU, Department of Periodontology, Laboratory of Oral Biomedical Science and Translational Medicine, School of Stomatology, Tongji University, Shanghai 200072, P.R. China. Tel: 86-21-66313739; Fax: 86-21-66524025. E-mail: hwliu@tongji.edu.cn.

This work was supported by grants from the National Natural Science Foundation of China (No. 30772418) and Shanghai Committee of Science and Technology (No. 074119514).

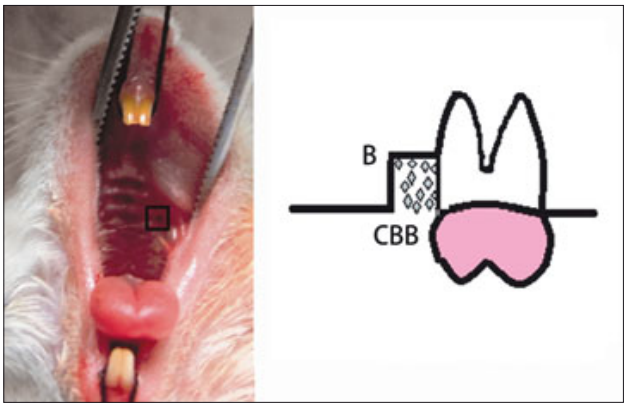

Fig 1 Image and diagrammatic illustration of the CPD. B: alveolar bone; CBB: ceramic bovine bone.

quently, we postulated that BMSCs were the precursor of PDLSCs in periodontal regeneration and this study was aimed to investigate this hypothesis *in vivo*.

Materials and methods

The protocols in this study were approved by the institutional review board and the Animal Care and Use Committee of Tongji University (Shanghai, China).

Animals

Male BALB/c mouse (aged 4–5 weeks) recipients were purchased from the Shanghai Laboratory Animal Centre (Shanghai, China). Male red fluorescent protein (RFP) mouse (aged 6 weeks) donors were a gift from the Shanghai Cancer Institute. Animals were housed in a pathogen-free barrier facility at the Animal Centre of Tongji University (Shanghai, China).

Chimera preparation

BALB/c recipients were subjected to whole body irradiation (8.5 Gy over 15 min). The BMSCs of RFP mice were obtained by flushing tibia and femur bones with phosphate buffered saline (PBS) (Gibco) and filtered through a sterile nylon mesh. Cells were centrifuged at 1,000 rpm for 3 min and resuspended at 10^7/ml. 1.0 x 10^7 RFP+ BMSCs were injected into BALB/c recipients via the tail vein at a concentration of 10^6 per 1 ml to establish an RFP^+ chimera model. Successful creation of the RFP^+ chimera was confirmed by demonstrating that RFP^+ peripheral blood mononuclear cells (PBMCs) in recipients had risen to 89% two months after transplantation.

Created periodontal defect (CPD)

After the successful creation of RFP^+ chimera, chimeric mice (N = 15) were anaesthetised with sodium pentobarbital. The gingival and palate mucosa on the mesial side of the left maxillary first molar were flapped to expose the alveolar bone overlying the mesial root. A three-wall defect (0.8–1.0 mm) was created using a steel round dental burr cooled with PBS. The defect was filled with pieces of ceramic bovine bone (CBB) (a gift from Second Military Medical University). Finally, the gingival flaps were repositioned and sutured using a 10-0 silk strand (Fig 1).

In vivo fluorescence imaging

Successfully transplanted BMSCs were tracked using an imaging system (IVIS spectrum, Caliper). A single untreated mouse was used as a negative control. Subsequently, chimeric mice were divided into three groups at random and observed 3, 14 and 28 days respectively after the creation of the periodontal defect. Mice were anaesthetised with isoflurane in an induction chamber prior to the imaging process.

Statistical analysis

RFP signals detected in chimeric mice (n = 15) were analysed using SPSS 12.0 software (SPSS. San Rafael, CA, USA). Data were presented as mean ± standard error of the mean (SEM). Differences among multiple experimental groups were evaluated by ANOVA for multiple comparisons. A *P* value of less than 0.05 was considered to indicate significant differences.

Haematoxylin and eosin staining and immunohistochemical analysis

Three groups of chimeric mice were sacrificed 3, 14 and 28 days after the creation of the periodontal defect respectively. Maxillae were removed and fixed in formalin for 24 h and then decalcified in ethylene diamine tetraacetic acid (EDTA-2Na) for 15 days at 4°C. Paraffin sections were used for haematoxylin and eosin (H&E) staining or immunohistochemical analysis. The periodontium of the right maxillary first molar was used as a control group. Specimens were sectioned in the mesial-distal plane. For immunohistochemical analysis, sections were first blocked in 10% normal goat serum in PBS for 30 min at room temperature and then incubated with primary rabbit anti-RFP antibody (1:150, CW Biotech), rat anti-mouse CD31 (1:150, Biolegend), rat

anti-mouse CD105 (1:150, Biolegend) or rat anti-mouse CD45 (1:150, Biolegend) at 4°C overnight. Sections were then incubated with HRP-conjugated secondary goat anti-rabbit antibody (1:500, Jackson) or goat-rat antibody (1:500, Jackson) at room temperature for 1 hour. Finally, sections were visualised using 3,3-diaminobenzidine tetrahydrochloride (DAB, Boster).

Results

Establishment of bone marrow transplantation model

Two months after transplantation, the frequency of RFP^+ PBMCs in recipients has risen to 89% (data not shown), therefore demonstrating that the model of bone marrow transplantation was successfully established. Furthermore, *in vivo* imaging revealed RFP signals across almost the entire body (Fig 2), with particularly strong signals detected in the forelimbs, which may be attributed to homing of a mass of BMSCs to the bone marrow of the tibia and femur. In contrast, only weak signals (attributed to interference) were detected in the negative control (far right image).

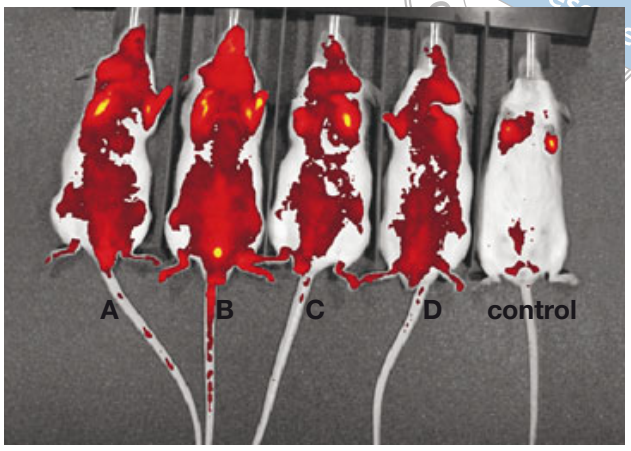

Fig 2 Signals detected by in vivo imaging system 2 months after bone marrow transplantation (BMT). A, B, C, D are chimeric mice treated with bone marrow transplatation. The far right image is the negative control mouse without any treatment.

RFP signals in the periodontal defect after transplantation

Red fluorescence was detected in the mesial region of the maxillary first molar on day 3, which indicated that RFP^+ cells had entered the defect. The intensity of the signal was stronger and the area was enlarged on day 14 compared with that on day 3. Moreover, this trend in increased area and intensity of the RFP+ signal continued to day 28. Unfortunately, the signal was not traced beyond this point (Fig 3).

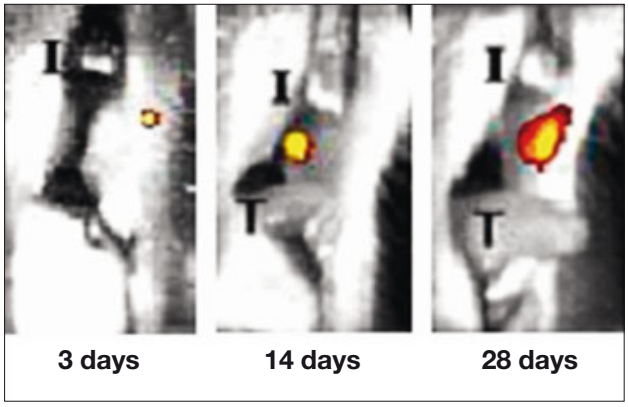

Fig 3 RFP signal in the periodontal defect observed 3, 14, and 28 days respectively after the creation of periodontal defect. I: maxillary incisor; T: tongue.

Signal value analysis

Statistical analysis revealed increased RFP signal with time in 28 days, with a rapid rise in intensity from day 3 to day 14 (Fig 4). Moreover, there were significant differences among three groups ($P < 0.05$).

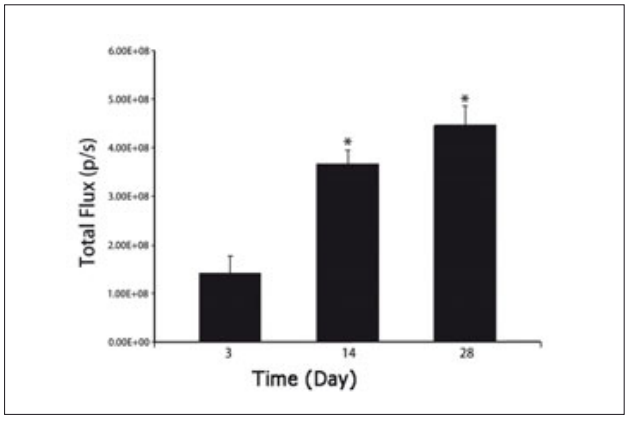

Fig 4 Analysis of RFP signal values after the creation of periodontal defect. There were significant differences among three groups.

H&E staining

H&E staining of periodontal tissue was performed and analysed after the creation of periodontal defect. On day 3, there was no newborn tissue among the CBB (Figs 5a and 5b). However, on day 28, space inside the CBB was filled with fibre-like structures and fibroblasts (Figs 5c and 5d).

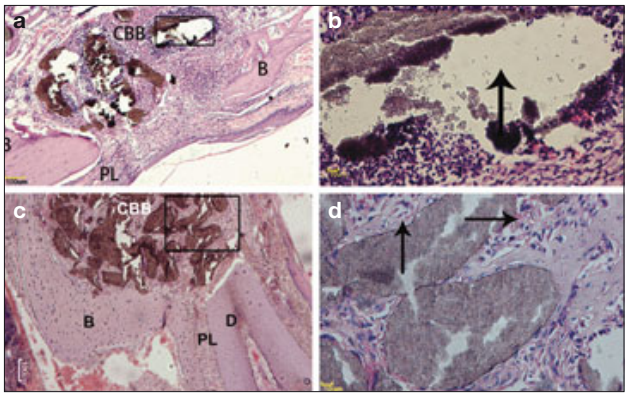

Fig 5 Diagram showing H&E staining of the periodontal defect on day 3 (**a** and **b**) and day 28 (**c** and **d**). **b** and **d** are magnified images of **a** and **c** respectively. (**a** and **b**) On day 3, there was no newborne tissue among CBB (black arrow). (**c** and **d**) However, on day 28, space inside CBB was filled with fiber-like structure and fibroblasts (black arrows). B: alveolar bone; D: dentine; CBB: ceramic bovine bone; PL: periodontal ligament.

Location of RFP$^+$ cells over time

Immunohistochemical analysis was conducted to investigate the involvement and location of RFP$^+$ BMSCs in periodontal repair. Increasing numbers of RPF$^+$ cells were detected with time after the creation of a periodontal defect. On day 3, only a small fraction of cells, located among the CBB, were positive for RFP (Figs 6a and 6b). Increasing numbers of RPF$^+$ cells migrated into the periodontal defect with a dispersed distribution in and around CBB on day 14 (Figs 6c and 6d). Although the location of RFP$^+$ cells at these two time points was limited to the CBB, a greater number and more extensive distribution of RPF$^+$ cells were observed on day 28 (Figs 6e to 6g). A mass of RFP$^+$ cells was observed outside the CBB, including areas surrounding the blood vessels (Fig 6g, transparent arrows). Furthermore, RFP$^+$ cells tended to accumulate near the alveolar bone

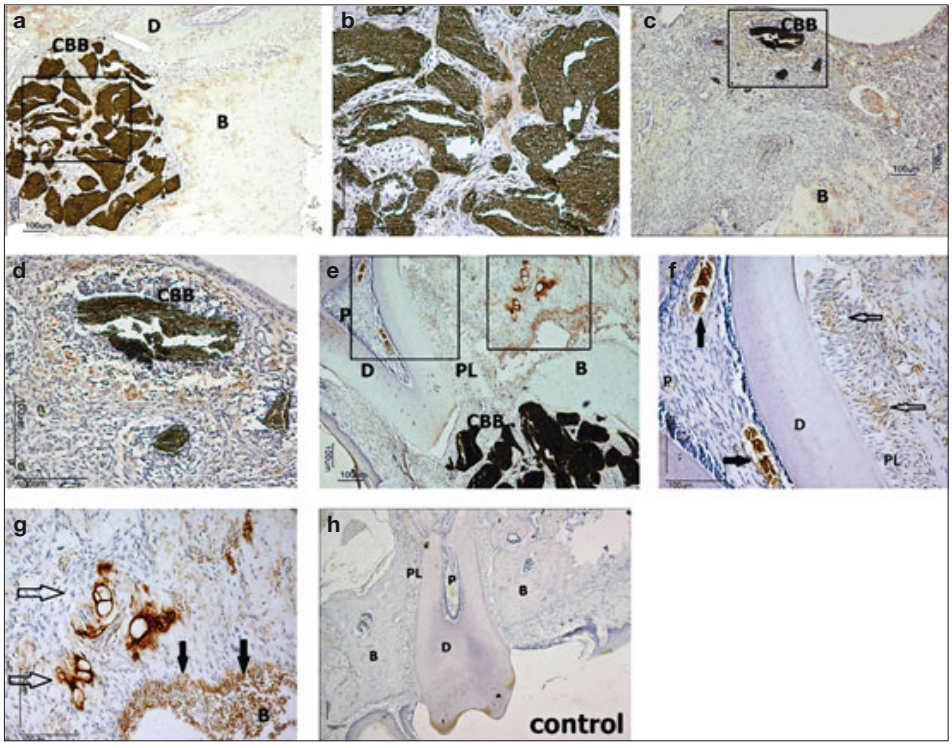

Fig 6 Immunohistochemical staining of RFP$^+$ cells in the periodontal defect on day 3 (**a** and **b**), day 14 (**c** and **d**) and day 28 (**e**, **f** and **g**). **b** and **d** are magnified images of **a** and **c** respectively. **f** and **g** are magnified images of **e**. **f** shows immunohistochemical staining of RFP$^+$ cells in normal periodontal tissue (control). (**a** and **b**) On day 3, only a small fraction of RFP$^+$ cells were located among the CBB (black arrows in **b**). (**c** and **d**) On day 14, increasing numbers of RPF$^+$ cells were observed in the periodontal defect with a dispersed distribution in and around the CBB (black arrows in **d**) (**e, f** and **g**) However, on day 28, a greater number and more extensive distribution of RPF$^+$ cells was observed (**g**). Cells were predominantly located around the blood vessels (transparent arrows), near the alveolar bone (black arrows), (**f**) and in the periodontal ligament (transparent arrows). (**f**) Moreover, RPF$^+$ cells were also found in the pulp (black arrows). B: alveolar bone; D: dentine; P: pulp; PL: periodontal ligament; CBB: ceramic bovine bone.

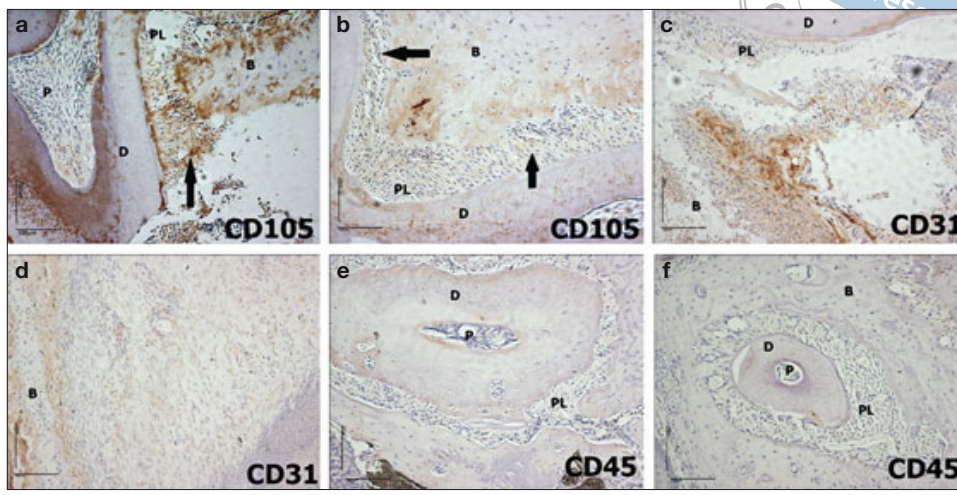

Fig 7 Cell surface marker analysis: CD105 (**a** and **b**), CD31 (**c** and **d**) and CD45 (**e** and **f**). **b, d** and **f** are control groups. (**A** and **B**) numerous CD105$^+$ cells were detected in the periodontal defect (black arrows in **a**), while relatively few cells were found in normal periodontal tissue (black arrows in **b**). (**c** and **d**) Fewer CD31$^+$ cells in normal tissue (black arrows in **d**) were detected than in the CPD (black arrows in **c**). (**e** and **f**) CD45$^+$ cells were not detected in either injured or healthy tissues. B: alveolar bone; D: dentine; P: pulp; PL: periodontal ligament.

(Fig 6g, black arrows) and in the PDL (Fig 6f, transparent arrows) and in the pulp of the maxillary first molar (Fig 6f, black arrows). No RFP$^+$ cells were observed in the control group.

Cell surface markers analysis

A large number of CD105$^+$ cells were detected in the periodontal defect, while relatively few cells were found in normal periodontal tissue (Fig 7a and 7b). Similarly, more CD31$^+$ cells were detected in defect compared with in normal defect (Figs 7c and 7d), while CD45$^+$ cells were not detected in either injured or healthy tissues (Figs 7e and 7f).

Discussion

Both *in vivo* fluorescence imaging and immunohistochemical analysis showed the increased number of RFP$^+$ cells with time from day 3 to day 28, which indicated more and more BMSCs recruited to participate in the periodontal repair. It was a strong proof for the hypothesis that BMSCs act as the role of precursor of PDLSCs in periodontal repair. In recent years, BMSCs were found contributing to the periodontal regeneration by many scholars with the way of cell injection *in situ* or *in vitro* experiments[12-14]. Our research, with an overall new method, found a similar result in living body.

In order to analyse the population of BMSCs involved in periodontal defects, cell surface markers were labelled in our search. In the periodontal defect, a large number of CD105$^+$ cells were detected, while almost no CD45$^+$ cells were found, which indicated no haemopoietic stem cells (HSCs) migrated into the defect. The population of BMSCs that were involved in periodontal repair might probably be mesenchymal stem cells (MSCs). As we know, BMSCs are mainly comprised of two populations of cells, HSCs and MSCs[15]. Both HSCs and MSCs possess a differentiation capability toward orofacial tissues. For example, MSCs are able to differentiate to form the periodontal tissue[12,13,16], the craniofacial bone[17,18] and the mandibular condyle[19], while HSCs can differentiate toward the buccal mucosa[20]. In this study, the origin of MSCs might come from two aspects. One was bone marrow-derived MSCs, which migrated into the periodontium after injury occurred, the other was dormant tissue resident MSCs activated due to this stimulus.

The distribution of RFP$^+$ BMSCs became more dispersed with time, mainly in the paravascular region, near the alveolar surface and within the PDL. This specific positioning indicated two points. Firstly, BMSC flowed into periodontal tissue probably through blood vessels, and then migrated near the alveolar surface and in the PDL[21,22]. Secondly, the PDL possesses asymmetrically distributed stem cells, on the alveolar bone surface and on the root surface. Stem cells on the alveolar bone surface exhibit strong proliferation capability and higher multilineage differentiation potential[23]. In our research, BMSCs were only found near the alveo-

lar bone surface, which might be the result that cells on the alveolar bone side evolved from adult BMSCs, while those on the root side developed during embryonic development[6-9].

Moreover, compared to normal tissue, more $CD31^+$ cells were detected around the vessel in defect, which might be attributed to the crosstalk between endothelial cells and BMSCs. The paravascular region exists as a "cell niche", which is similar to that of stem cells. Signals in the niche stimulate the self-renewal, proliferation, differentiation and apoptosis of stem cells[24].

In this study, we firstly used *in vivo* imaging system in dental research area for tracing labelled cells. This non-lethal conditioning approach as well as the establishment of BMT model provided new methodology for observing the role of BMSC in periodontal regeneration in the future study.

Conclusion

Bone marrow derived stem cells were shown to migrate to the periodontal injury *in vivo* without lethal conditioning. Increasing numbers of BMSCs were detected during 28 days after the creation of periodontal defect, which tended to accumulate around blood vessels and near alveolar bone. Greater number of $CD105^+$ and $CD31^+$ cells were detected in defective periodontium compared with normal tissue. Furthermore, the presence of $CD105^+$ cells and the absence of $CD45^+$ cells indicated that MSCs participated in periodontal regeneration, while HSCs did not.

References

1. Pihlstrom BL, Michalowicz BS, Johnson NW. Periodontal diseases. Lancet 2005;366:1809–1820.
2. Bratthall G, Soderholm G, Neiderud AM et al. Guided tissue regeneration in the treatment of human infrabony defects. Clinical, radiographical and microbiological results: a pilot study. J Clin Periodontol 1998;25:908–914.
3. Lang H, Schuler N, Nolden R. Attachment formation following replantation of cultured cells into periodontal defects--a study in minipigs. J Dent Res 1998;77:393–405.
4. Langer R, Vacanti JP. Tissue engineering. Science 1993;260:920–926.
5. Seo BM, Miura M, Gronthos S et al. Investigation of multipotent postnatal stem cells from human periodontal ligament. Lancet 2004;364:149–155.
6. Moore WJ. The periodontium. handbook of microscopic anatomy. J Anat 1987;154:267.
7. Cho MI, Garant PR. Ultrastructural evidence of directed cell migration during initial cementoblast differentiation in root formation. J Periodontal Res 1988;23:268–276.
8. Cho MI, Garant PR. Radioautographic study of [3H]mannose utilization during cementoblast differentiation, formation of acellular cementum, and development of periodontal ligament principal fibers. Anat Rec 1989;223:209–222.
9. Cho MI, Garant PR. Development and general structure of the periodontium. Periodontol 2000 2000;24:9–27.
10. Shi S, Gronthos S. Perivascular niche of postnatal mesenchymal stem cells in human bone marrow and dental pulp. J Bone Miner Res 2003;18:696–704.
11. Nagatomo K, Komaki M, Sekiya I et al. Stem cell properties of human periodontal ligament cells. J Periodontal Res 2006;41:303–310.
12. Kawaguchi H, Hirachi A, Hasegawa N et al. Enhancement of periodontal tissue regeneration by transplantation of bone marrow mesenchymal stem cells. J Periodontol 2004;75:1281–1287.
13. Kawaguchi H, Hayashi H, Mizuno N et al. Cell transplantation for periodontal diseases. A novel periodontal tissue regenerative therapy using bone marrow mesenchymal stem cells. Clin Calcium 2005;15:99–104.
14. Hasegawa N, Kawaguchi H, Hirachi A et al. Behavior of transplanted bone marrow-derived mesenchymal stem cells in periodontal defects. J Periodontol 2006;77:1003–1007.
15. Smith A. Glossary A glossary for stem-cell biology. Nature 2006;441:1060.
16. Yang Z, Jin F, Zhang X et al. Tissue engineering of cementum/periodontal-ligament complex using a novel three-dimensional pellet cultivation system for human periodontal ligament stem cells. Tissue Eng Part C Methods 2009;15:571–581.
17. Abukawa H, Shin M, Williams WB et al. Reconstruction of mandibular defects with autologous tissue-engineered bone. J Oral Maxillofac Surg 2004;62:601–606.
18. De Kok IJ, Drapeau SJ, Young R et al. Evaluation of mesenchymal stem cells following implantation in alveolar sockets: a canine safety study. Int J Oral Maxillofac Implants 2005;20:511–518.
19. Abukawa H, Terai H, Hannouche D et al. Formation of a mandibular condyle in vitro by tissue engineering. J Oral Maxillofac Surg 2003;61:94–100.
20. Tran SD, Pillemer SR, Dutra A et al. Differentiation of human bone marrow-derived cells into buccal epithelial cells in vivo: a molecular analytical study. Lancet 2003;361:1084–1088.
21. Gould TR, Melcher AH, Brunette DM. Migration and division of progenitor cell populations in periodontal ligament after wounding. J Periodontal Res 1980;15:20–42.
22. McCulloch CA, Nemeth E, Lowenberg B et al. Paravascular cells in endosteal spaces of alveolar bone contribute to periodontal ligament cell populations. Anat Rec 1987;219:233–242.
23. Wang L, Shen H, Zheng W et al. Characterization of stem cells from alveolar periodontal ligament. Tissue Eng Part A 2011;17:1015–1026.
24. Jones DL, Wagers AJ. No place like home: anatomy and function of the stem cell niche. Nat Rev Mol Cell Biol 2008;9:11–21.